ACS OMEGA

http://pubs.acs.org/journal/acsodf

Article

Ulex Europaeus Agglutinin-I-Based Magnetic Isolation for the Efficient and Specific Capture of SW480 Circulating Colorectal Tumor Cells

Rongrong Tian, Xiaodong Li, Hua Zhang, Lina Ma, Huimao Zhang,* and Zhenxin Wang*

Cite This: *ACS Omega* 2022, 7, 30405−30411

Read Online

ACCESS | Metrics & More | Article Recommendations | Supporting Information

ABSTRACT: The efficient and specific capture of circulating tumor cells (CTCs) from patients' peripheral blood is of significant value in precise cancer diagnosis and cancer therapy. As fine targeting molecules, lectins can recognize cancer cells specifically due to the abnormal glycosylation of molecules on the cancer cell membrane and the specific binding of lectin with glycoconjugates. Herein, a Ulex europaeus agglutinin-I (UEA-I)-based magnetic isolation strategy was developed to efficiently and specifically capture α-1,2-fucose overexpression CTCs from colorectal cancer (CRC) patients' peripheral blood. Using UEA-I-modified Fe_3O_4 magnetic beads (termed MB-UEA-I), up to 94 and 89% of target cells (i.e., SW480 CRC cells) were captured from the cell spiking complete cell culture medium and whole blood, respectively. More than 90% of captured cells show good viability and proliferation ability without detaching from MB-UEA-I. In combination with three-color immunocytochemistry (ICC) identification, MB-UEA-I has been successfully used to capture CTCs from CRC patients' peripheral blood. The experimental results indicate a correlation between CTC characterization and tumor metastasis. Specifically, MB-UEA-I can be applied to screen early CRC by capturing CTCs when served as a liquid biopsy. The presented work offers a new insight into developing cost-effective lectin-functionalized methods for biomedical applications.

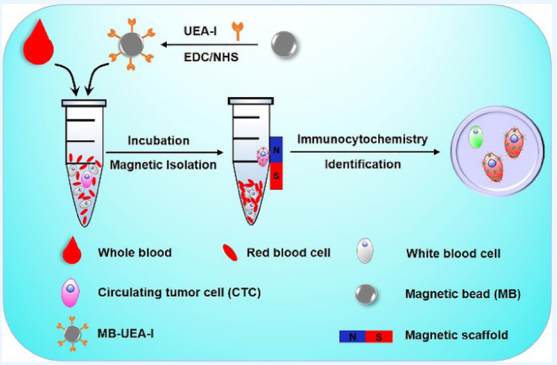

INTRODUCTION

Circulating tumor cells (CTCs) refer to a general term for various types of tumor cells shed from the primary site into peripheral blood with the ability to metastasize to distant organs and form metastatic tumors.[1−3] Thus, capturing and detecting CTCs may hold great clinical significance for noninvasive tumor profiling, efficacy monitoring, prognosis prediction, and early diagnosis of metastasis like a liquid biopsy.[4−6] Nevertheless, efficient enrichment of high-purity CTCs is a tremendous challenge because of high heterogeneity and intrinsic rarity. Generally, there are only a few-to-several hundred CTCs in 10^6−10^9 hematologic cells per milliliter of peripheral blood.[7,8]

To date, researchers have developed numerous methods to highly efficiently capture and detect CTCs, which are mostly in view of their physical properties (density, size, deformability, and adhesion preference)[9−13] and/or biological characteristics (antibody−antigen, aptamer, peptides, and E-selectin).[14−34] For instance, a microfluidic immunoaffinity assay for CTC isolation from breast cancer patients' blood was proposed by Park et al.[18] The related isolation strategy obviously improves both capture efficiency and recovery of the isolated CTCs, which is very important for performing sensitive downstream assays. Wu et al. designed an efficient and reliable multifunctional nanosphere system with chip assistance for biomarker phenotyping of single heterogeneous CTCs based on the size and specific targeting of human epidermal growth factor receptor 2 (HER2) and the epithelial cell adhesion molecule (EpCAM).[19] A signal amplification detection method based on Ag_2S fluorescent nanodots combined with immunomagnetic spheres (IMNs) was proposed by Ding et al., which has been used for the magnetic capture of CTCs with high efficiency (six CTCs per milliliter of the mimic whole blood) as well as ultrasensitive fluorescence labeling.[20] Especially, CTC enrichment based on antibody (e.g., epidermal growth factor receptor (EGFR), EpCAM, HER2, etc.)-modified immunomagnetic beads are the most commonly applied for CTC isolation from the peripheral blood of patients.[25−30] This magnetic isolation method shows several advantages including simple magnetic operation, specific and effective coupling with target cells, and easy integration with consecutive identification and analysis (such as immunocytochemistry (ICC) and Raman imaging). Importantly, the CellSearch system based on

Received: June 14, 2022
Accepted: August 8, 2022
Published: August 17, 2022

Scheme 1. Schematic Illustration of CTC Capture and Identification Based on MB-UEA-I

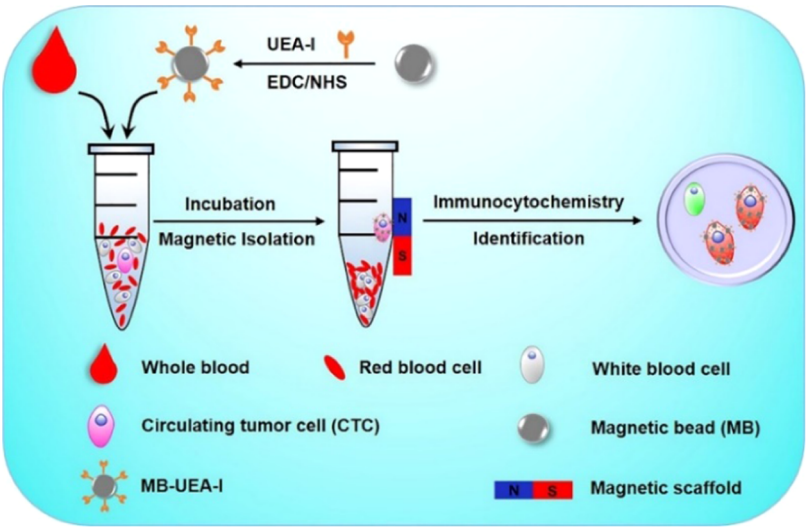

magnetic isolation has been approved by the U.S. Food and Drug Administration (FDA), which is used to assess the diagnostic and prognostic efficacy in patients with metastatic colorectal cancer, breast cancer, and prostate cancer.[31,32]

Despite the fact that antibody functionalization has highly improved CTC capture efficiency, the antibody-dependent CTC isolation strategy remains limited in widespread clinical applications due to its bench-to-bench stability, reproducibility, mass production, and high cost.[5,35,36] Besides, antibodies (such as EpCAM) expressed on the surface of CTCs are probably more heterogeneous than initially expected (that is, the epithelial−mesenchymal transition (EMT) leads to not only the decreased expression of epithelial markers (EpCAM) but also increased expression of mesenchymal markers (EGFR))[5,37] and are even missing in certain tumor classes (e.g., sarcoma and melanoma).[38] Thus, other targeting molecules, like DNA aptamers,[39,40] recognition peptides,[41] or specific binding lectins,[42,43] have also been tested in CTC isolation. Compared to antibodies, lectins are ubiquitous in a variety of plants including beans and grains, which are amenable to mass production and play important roles in identification of glycoprotein and the phase of the disease. They have been widely used in cytochemistry, histochemistry, and immunochemistry for the detection and characterization of glycosylated residues and different glycoconjugates in human or animal cells and tissue surfaces.[44,45] For instance, Xie et al. put forward trifunctional nanospheres modified with wheat germ agglutinin to identify DU-145 cells with sialic acid and *N*-acetylglucosamine expressed on the surface.[42] Therefore, the lectin-modified magnetic isolation strategy could be a promising technique for CTC isolation. Our previous work demonstrates that Ulex europaeus agglutinin-I (UEA-I) can conjugate with α-1,2-fucose on the surface of SW480 cells effectively and selectively[46,47] and thus shows potential for the early diagnosis of colorectal cancer (CRC) as well as cancer phenotype identification as a biomarker.

Herein, a cell-sorting strategy is proposed to efficiently capture and isolate CTCs, which is based on UEA-I-modified Fe_3O_4 magnetic beads (termed MB-UEA-I). The resulting MB-UEA-I can capture SW480 cells spiked in peripheral blood highly efficiently. In addition, the captured cells show good viability, which satisfies requirements for downstream mutation detection and cell proliferation. Furthermore, the practicability of MB-UEA-I is demonstrated by CTC capture and isolation from unprocessed CRC patients' blood samples. This work also identifies that primary CRC and metastatic CRC have different CTC characterization.

EXPERIMENTAL SECTION

Preparation of MB-UEA-I. The carboxyl group of MBs was activated for conjugation with UEA-I through covalent attachment to obtain MB-UEA-I. The experimental details are illustrated in the Supporting Information (SI).

Capturing SW480 Cells in Cell Spiking Samples. One hundred SW480 cells were spiked into 1 mL of complete culture medium (L-15 + 10 v%/v% FBS) and incubated with 0.05 mg of MB-UEA-I at 37 °C with gentle shaking for 45 min. Subsequently, an external magnet was used to separate the MB-UEA-I-captured cells, while the uncaptured cells in supernatants were transferred into a 48-well plate and counted by an inverted microscope. As control experiments, 0.05 mg of MB-UEA-I or blank MBs were incubated with 100 HCT116 cells, 100 NCM460 cells, or 100 SW480 cells spiked in 1 mL of complete culture medium, separately, and the captured cells were separated and counted as previously described. Besides, the Hoechst 33342-prestained SW480 cells, Rhodamine B-prestained HCT116 cells, and Rhodamine B-prestained NCM460 cells were also incubated with MB-UEA-I or blank MBs. After separation, the captured and uncaptured cells were observed via a fluorescence microscope. In addition, MB-UEA-I or MBs after interactions with cells were also observed through scanning electron microscopy (SEM) characterization.

For investigating the capture sensitivity of MB-UEA-I toward SW480 cells, various amounts of SW480 cells were spiked into 1 mL of complete culture medium (L-15 + 10 v %/v% FBS) and incubated with 0.05 mg of MB-UEA-I at 37 °C with gentle shaking for 45 min. After separation, the uncaptured cells in supernatants were transferred into a 48-well plate and counted by an inverted microscope. Furthermore, the capture sensitivity of MB-UEA-I toward SW480 cells spiking in the whole blood sample was also investigated. Various amounts of Hoechst 33342-prestained SW480 cells were spiked into 1 mL of the fresh healthy blood sample. The capture process was

https://doi.org/10.1021/acsomega.2c03702
ACS Omega 2022, 7, 30405−30411

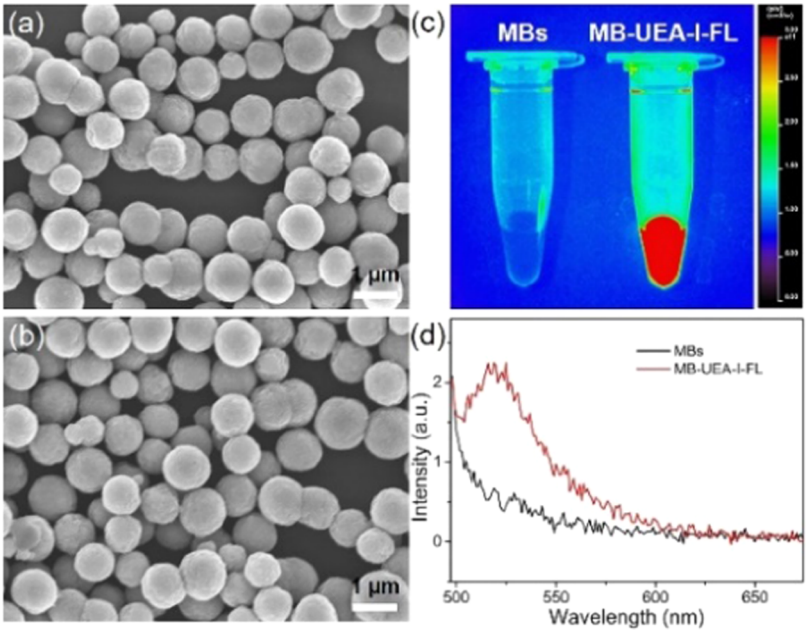

Figure 1. SEM micrographs of (a) MBs and (b) MB-UEA-I, and the fluorescence images (c) and fluorescence spectra (d) of MBs and MB-UEA-I-FL.

carried out as mentioned above but the MB-UEA-I-captured cells were characterized via a fluorescence microscope.

Cell Viability and Proliferation Study. Calcein AM and propidium iodide (PI) were chosen to study the cell viability, while the proliferation study was conducted by reculturing the MB-UEA-I-captured SW480 cells (see the SI for experimental details).

Capture and ICC Identification of SW480 and CTC Cells. The mimic clinical sample was obtained by spiking 10 SW480 cells into 1 mL of the healthy whole blood. Then, 0.05 mg of MB-UEA-I were added to the sample, incubated under gentle shaking at 37 °C for 45 min, and subsequently separated by an external magnet. The three-color ICC was used to recognize MB-UEA-I-captured cells. For the clinical practicability test, blood samples collected from 14 CRC patients before surgery and 5 healthy individuals were separately incubated with 0.05 mg of MB-UEA-I to capture CTCs, which were further identified by ICC.

RESULTS AND DISCUSSION

Preparation and Characterization of MBs and MB-UEA-I. As shown in Scheme 1, UEA-I was modified on the surface of MBs by carbodiimide chemistry through covalent attachment. The as-obtained MB-UEA-I can specifically recognize α-1,2-fucose positive cancer cells, such as SW480 cells and CTCs of primary CRC. The average size of MBs is 1.02 ± 0.06 μm in diameter. After being modified with UEA-I, the MBs exhibit a negligible change in morphology and dispersibility (as shown in Figure 1a,b). To confirm the combination of MBs with UEA-I, FL-UEA-I was employed to react with MBs. Under 488 nm excitation, MB-UEA-I-FL emits an obvious fluorescence at 520 nm (as shown in Figure 1c,d). Besides, we figured out the calibration curve of FL-UEA-I and measured the fluorescence spectra of 25 μg of FL-UEA-I before and after reaction with 0.5 mg of MBs. According to the change in fluorescence intensity, we found that the coupling quantity of FL-UEA-I on MBs was about 16 μg mg^{-1} (as shown in Figure S1).

Specific Capture of SW480 Cells with MB-UEA-I. The concentration of MB-UEA-I and incubation time were optimized to obtain the maximum capture efficiency. Figure S2a shows that the capture efficiency increases as the concentration of MB-UEA-I increases. More than 90% of spiked SW480 cells are captured when the concentration of MB-UEA-I is higher than 0.05 mg mL^{-1}. In addition, as the incubation time of MB-UEA-I with cells increases, the capture efficiency also increases and more than 90% of SW480 cells can be captured when the incubation time is longer than 45 min (as shown in Figure S2b). Considering that a higher concentration of MB-UEA-I and longer incubation time may result in more nonspecific capture of untargeted cells, 0.05 mg mL^{-1} MB-UEA-I and an incubation time of 45 min are chosen to capture targeted cells in the following experiments.

For testing their specificity, MB-UEA-I were first incubated with two CRC cell lines (SW480 cells and HCT116 cells) and one normal colorectal cell line (NCM460 cells) under the optimized conditions. In comparison with HCT116 and NCM460 cells, SW480 cells express α-1,2-fucose residues on the cell membrane surface with an aberrantly high level, which have a high binding affinity with UEA-I through the combination with α-1,2-fucosylated lactodifucotetraose-derived neoglycolipid.[46−48] As expected, MB-UEA-I can capture more than 94% of spiked SW480 cells in complete culture medium, which is much higher than those of spiked HCT116 cells (12%) and NCM460 cells (11%) (as shown in Figure 2). Moreover, few SW480 cells were captured by the unmodified MBs. Besides, the fluorescence imaging studies of MB-UEA-I- or MB-treated cells also verify the specific binding between MB-UEA-I and SW480 cells (Figure S3). The SEM micrographs in Figure S4 also show the successful attachment of MB-UEA-I on the SW480 cell surface. The results suggest that MB-UEA-I can be used to efficiently and specifically capture SW480 cells.

Capturing SW480 Cells Spiked in Mimic CTC Samples. Different amounts (ranging from 3 to 1000) of SW480 cells were added to 1 mL of complete culture medium

https://doi.org/10.1021/acsomega.2c03702
ACS Omega 2022, 7, 30405−30411

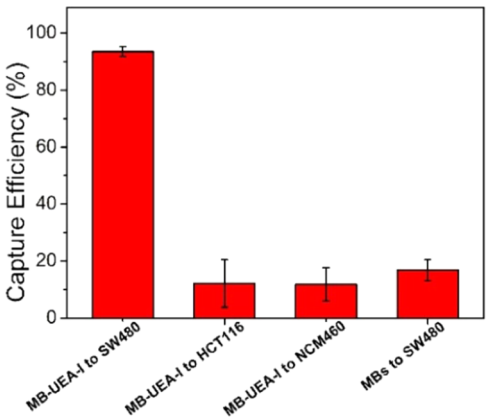

Figure 2. Capture efficiencies of MB-UEA-I to SW480 cells, HCT116 cells, and NCM460 cells, and the capture efficiency of MBs to SW480 cells. Error bars mean standard deviations (SD, n = 3).

or healthy whole blood to investigate the capture sensitivity of MB-UEA-I. Under the optimal experimental conditions, the calibration curves were obtained by plotting the linearity of the captured cell numbers against the spiked cell numbers. As shown in Figure 3a, the linear equations are $y_1 = 0.94x - 0.92$ ($R^2 = 0.9998$) for SW480 cells in complete culture medium and $y_2 = 0.89x + 0.08$ ($R^2 = 0.9987$) for SW480 cells in the whole blood, indicating that capture sensitivity are 94 and 89% in complete culture medium and whole blood, respectively. In particular, four SW480 cells were captured from six SW480 cells spiking 5 mL of whole blood (as shown in Figure S5), demonstrating the high capture sensitivity of MB-UEA-I. These results reveal that the as-constructed MB-UEA-I can be directly applied to sort CTCs of primary CRC in clinical samples. Furthermore, the captured cells from SW480 cells spiking the whole blood were identified with ICC by the use of Hoechst 33342 (a marker for nucleus), Alexa Fluor 488-labeled anti-CK19 (a marker for epithelial cells) monoclonal antibody, and Alexa Fluor 594-labeled anti-CD45 (a marker for white blood cells (WBCs)) monoclonal antibody.[49] Hoechst $33342^+/CK19^+/CD45^-$ cells are recognized as SW480 cells, while Hoechst $33342^+/CK19^-/CD45^+$ are sorted as WBCs. As shown in Figure 3b, SW480 cells and WBCs can be effectively separated by MB-UEA-I. The result confirms that the cell-sorting method based on MB-UEA-I enables efficient and reliable detection of CTCs.

Cell Viability Analysis and Proliferation Study. The viability of MB-UEA-I-captured SW480 cells was analyzed through Calcein AM and PI costaining. Most captured cells exhibit green fluorescence emission, and the viability rate is calculated to be 93%, which is similar to the viability rate (95%) of the control cells (Figure S6). Besides, the proliferation ability of MB-UEA-I-captured cells was further explored. The captured cells with MB-UEA-I on the surface can well adhere to the culture plates and exhibit strong proliferation ability (as shown in Figure 4). In particular, the proliferation rate of MB-UEA-I-captured SW480 cells is as rapid as that of normal cultured SW480 cells (Figure S7). The results distinctly illustrated that the captured cells retained both the cell viability and proliferative ability, enabling trusty downstream studies, for example, gene expression, mutation, sequencing, etc.

CTC Capture and Identification from Clinical CRC Patients' Peripheral Blood. The clinical practicability of MB-UEA-I was demonstrated by directly profiling CTCs in peripheral blood samples, which were collected from 14 CRC patients before surgery and 5 healthy individuals. The Hoechst $33342^+/CK19^+/CD45^-$ cells characterized by ICC were classified as CTCs. As illustrated in Figure 5a and Table S1, the CTC numbers ranged from 3 to 20 cells mL^{-1} blood from CRC patients, while there are no CTCs in the blood samples of healthy donors. As a typical sample, the fluorescence images of 16 CTCs captured from the blood sample of the No. 5 patient are shown in Figure 5b. In addition, the numbers of CTCs (mean values of 13 ± 4 CTCs mL^{-1}) in blood samples from primary CRC patients (nos. 1−7) are higher than that in blood samples (mean values of 5 ± 2 CTCs mL^{-1}) from metastatic CRC patients (nos. 8−14). The phenomenon is caused by decreasing the fucosylation level of the CRC cell membrane with tumor progression, i.e., the cell membrane is highly fucosylated at an early stage of CRC and gradually defucosylated through genetic mutation in the metastasis stage of CRC.[50] The result indicates the characterization of CTCs associated with disease progression and demonstrates that the MB-UEA-I-based magnetic isolation strategy is a promising tool for the early diagnosis of CRC. But it still needs to be combined with other diagnostic techniques to determine the CRC stage accurately.

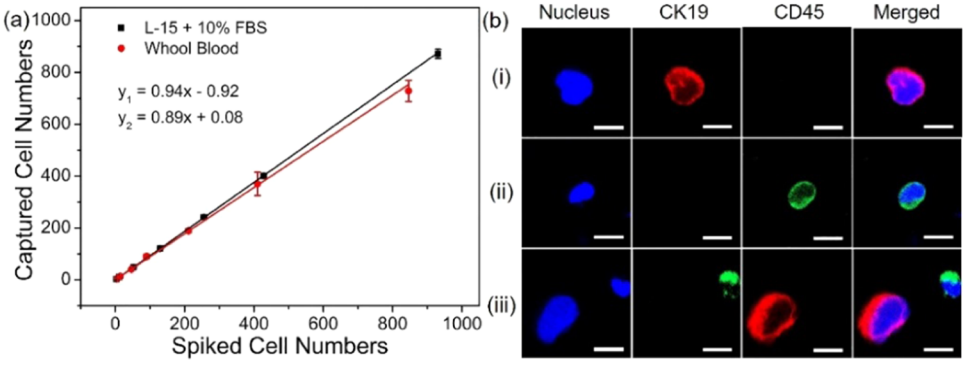

Figure 3. (a) Capture sensitivities of MB-UEA-I to SW480 cells. Error bars mean SD (n = 3). (b) Typical fluorescence images of the cells identified by ICC ((i) SW480 cells spiking the whole blood sample, (ii) WBC in the supernatant, and (iii) MB-UEA-I-captured SW480 cells). Scale bars are 10 μm.

https://doi.org/10.1021/acsomega.2c03702
ACS Omega 2022, 7, 30405−30411

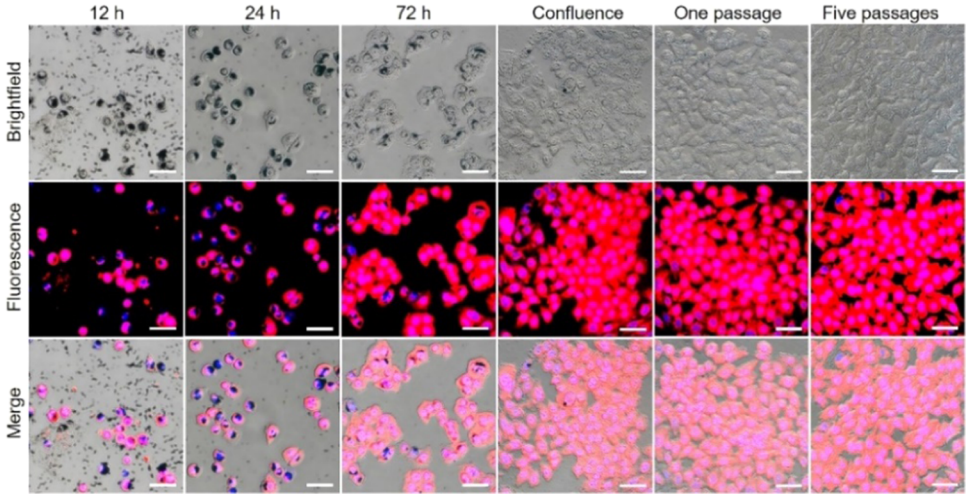

Figure 4. Fluorescence images of MB-UEA-I-captured SW480 cells after re-cultured. From left to right: adhered to the plate, proliferated, just reached confluence, reached confluence after one passage and five passages, respectively. The scale bars are 50 μm.

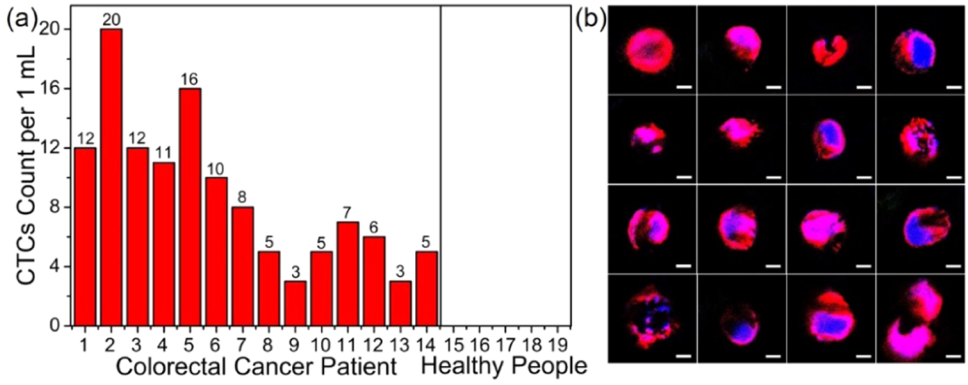

Figure 5. (a) Quantitative detection of CTCs from 14 CRC patients (nos. 1−14) and 5 healthy individuals (nos. 15−19) blood samples. (b) Fluorescence images of the MB-UEA-I-captured CTCs from patient no. 5 by three-color ICC identification. Scale bars are 5 μm.

CONCLUSIONS

In summary, a convenient and rapid lectin-based magnetic isolation strategy is developed to highly efficiently and specifically capture CTCs of CRC through strong binding affinity between UEA-I and α-1,2-fucose. The captured cells are completely suitable for downstream studies such as CTC culture, gene expression, and mutation detection because the as-proposed MB-UEA-I magnetic isolation platform exhibits a negligible effect on cell viability and proliferation ability. Heterogeneous populations/features of CTCs at different disease progression stages have been demonstrated by profiling CTCs in whole blood samples from 14 CRC patients, which may offer helpful information for clinical decisions. Therefore, the lectin-based magnetic isolation strategy demonstrates the practical use of lectin-based isolation of rare cells and has a great promise to be translated to the clinic as a cost-effective liquid biopsy method.

ASSOCIATED CONTENT

Supporting Information

The Supporting Information is available free of charge at https://pubs.acs.org/doi/10.1021/acsomega.2c03702.

Experimental section; optimization of MB-UEA-I concentration and incubation time; SEM observation; ICC identification; and table of CTC capture numbers from 19 clinical peripheral blood samples (PDF)

AUTHOR INFORMATION

Corresponding Authors

Huimao Zhang − *Department of Radiology, The First Hospital of Jilin University, Changchun, Jilin 130021, P. R. China*; Email: huimao@jlu.edu.cn

Zhenxin Wang − *State Key Laboratory of Electroanalytical Chemistry, Changchun Institute of Applied Chemistry, Chinese Academy of Sciences, Changchun 130022, P. R. China; University of Science and Technology of China, Hefei, Anhui 230026, P. R. China*; orcid.org/0000-0002-1908-9848; Email: wangzx@ciac.ac.cn

Authors

Rongrong Tian − *State Key Laboratory of Electroanalytical Chemistry, Changchun Institute of Applied Chemistry, Chinese Academy of Sciences, Changchun 130022, P. R. China; University of Science and Technology of China, Hefei, Anhui 230026, P. R. China*

Xiaodong Li − *Department of Radiology, The First Hospital of Jilin University, Changchun, Jilin 130021, P. R. China*

Hua Zhang − *State Key Laboratory of Electroanalytical Chemistry, Changchun Institute of Applied Chemistry,*

https://doi.org/10.1021/acsomega.2c03702
ACS Omega 2022, 7, 30405−30411

Chinese Academy of Sciences, Changchun 130022, P. R. China; orcid.org/0000-0001-7451-2058

Lina Ma − *State Key Laboratory of Electroanalytical Chemistry, Changchun Institute of Applied Chemistry, Chinese Academy of Sciences, Changchun 130022, P. R. China*

Complete contact information is available at: https://pubs.acs.org/10.1021/acsomega.2c03702

Notes

The authors declare no competing financial interest.

■ ACKNOWLEDGMENTS

This work was supported by the National Natural Science Foundation of China (Grant Nos. 21974133 and 81871406).

■ REFERENCES

(1) Plaks, V.; Koopman, C. D.; Werb, Z. Circulating tumor cells. *Science* **2013**, *341*, 1186−1188.

(2) Alix-Panabières, C.; Pantel, K. Opinion challenges in circulating tumour cell research. *Nat. Rev. Cancer* **2014**, *14*, 623−631.

(3) Ganesh, K.; Massagué, J. Targeting metastatic cancer. *Nat. Med.* **2021**, *27*, 34−44.

(4) Cristofanilli, M.; Budd, G. T.; Ellis, M. J.; Stopeck, A.; Matera, J.; Miller, M. C.; Reuben, J. M.; Doyle, G. V.; Allard, W. J.; Terstappen, L. W.; Hayes, D. F. N. Circulating tumor cells, disease progression, and survival in metastatic breast cancer. *N. Engl. J. Med.* **2004**, *351*, 781−791.

(5) Shen, Z.; Wu, A.; Chen, X. Current detection technologies for circulating tumor cells. *Chem. Soc. Rev.* **2017**, *46*, 2038−2056.

(6) Wu, L.; Wang, Y.; Xu, X.; Liu, Y.; Lin, B.; Zhang, M.; Zhang, J.; Wan, S.; Yang, C.; Tan, W. Aptamer-based detection of circulating targets for precision medicine. *Chem. Rev.* **2021**, *121*, 12035−12105.

(7) Wang, S.; Liu, K.; Liu, J.; Yu, Z. T. F.; Xu, X.; Zhao, L.; Lee, T.; Lee, E. K.; Reiss, J.; Lee, Y. K.; Chung, L. W. K.; Huang, J.; Retting, M.; Seligson, D.; Duraiswamy, K. N.; Shen, C. K. F.; Tseng, H. R. Highly efficient capture of circulating tumor cells by using nanostructured silicon substrates with integrated chaotic micromixers. *Angew. Chem., Int. Ed.* **2011**, *50*, 3084−3088.

(8) Ignatiadis, M.; Sledge, G. W.; Jeffrey, S. S. Liquid biopsy enters the clinic — implementation issues and future challenges. *Nat. Rev. Clin. Oncol.* **2021**, *18*, 297−312.

(9) Hofman, V. J.; Ilie, M. I.; Bonnetaud, C.; Selva, E.; Long, E.; Molina, T.; Vignaud, J. M.; Flejou, J. F.; Lantuejoul, S.; Piaton, E.; Butori, C.; Mourad, N.; Poudenx, M.; Bahadoran, P.; Sibon, S.; Guevara, N.; Santini, J.; Venissac, N.; Mouroux, J.; Vielh, P.; Hofman, P. M. Cytopathologic detection of circulating tumor cells using the isolation by size of epithelial tumor cell method promises and pitfalls. *Am. J. Clin. Pathol.* **2011**, *135*, 146−156.

(10) Park, J. M.; Lee, J. Y.; Lee, J. G.; Jeong, H.; Oh, J. M.; Kim, Y. J.; Park, D.; Kim, M. S.; Lee, H. J.; Oh, J. H.; Lee, S. S.; Lee, W. Y.; Huh, N. Highly efficient assay of circulating tumor cells by selective sedimentation with a density gradient medium and microfiltration from whole blood. *Anal. Chem.* **2012**, *84*, 7400−7407.

(11) Chen, W.; Weng, S.; Zhang, F.; Allen, S.; Li, X.; Bao, L.; Lam, R. H. W.; Macoska, J. A.; Merajver, S. D.; Fu, J. Nanoroughened surfaces for efficient capture of circulating tumor cells without using capture antibodies. *ACS Nano* **2013**, *7*, 566−575.

(12) Jiang, W.; Han, L.; Yang, L.; Xu, T.; He, J.; Peng, R.; Liu, Z.; Zhang, C.; Yu, X.; Jia, L. Natural fish trap-like nanocage for label-free capture of circulating tumor cells. *Adv. Sci.* **2020**, *7*, No. 2002259.

(13) Cheng, S.-B.; Wang, M.; Zhang, C.; Chen, M.-M.; Wang, Y.-K.; Tian, S.; Zhan, N.; Dong, W.-G.; Xie, M.; Huang, W.-H. Flexible three-dimensional net for intravascular fishing of circulating tumor cells. *Anal. Chem.* **2020**, *92*, 5447−5455.

(14) Yin, C.; Wang, Y.; Ji, J.; Cai, B.; Chen, H.; Yang, Z.; Wang, K.; Luo, C.; Zhang, W.; Yuan, C.; Wang, F. Molecular profiling of pooled circulating tumor cells from prostate cancer patients using a dual-antibody-functionalized microfluidic device. *Anal. Chem.* **2018**, *90*, 3744−3751.

(15) Zhai, T.-T.; Ye, D.; Zhang, Q.; Wu, Z.; Xia, X. Highly efficient capture and electrochemical release of circulating tumor cells by using aptamers modified gold nanowire arrays. *ACS Appl. Mater. Interfaces* **2017**, *9*, 34706−34714.

(16) Lu, N.-N.; Xie, M.; Wang, J.; Lv, S.; Yi, J.; Dong, W.; Huang, W. Biotin-triggered decomposable immunomagnetic beads for capture and release of circulating tumor cells. *ACS Appl. Mater. Interfaces* **2015**, *7*, 8817−8826.

(17) Wang, Z.; Wu, Z.; Ding, P.; Sun, N.; Feng, S.; Xing, C.; Zou, H.; Pei, R. Selective capture of circulating tumor cells by antifouling nanostructure substrate made of hydrogel nanoparticles. *Colloid Surf., B* **2021**, *202*, No. 111669.

(18) Park, M. H.; Reátegui, E.; Li, W.; Tessier, S. N.; Wong, K. H. K.; Jensen, A. E.; Thapar, V.; Ting, D.; Toner, M.; Stott, S. L.; Hammond, P. T. Enhanced isolation and release of circulating tumor cells using nanoparticle binding and ligand exchange in a microfluidic chip. *J. Am. Chem. Soc.* **2017**, *139*, 2741−2749.

(19) Wu, L.-L.; Tang, M.; Zhang, Z.; Qi, C.; Hu, J.; Ma, X.; Pang, D. Chip-assisted single-cell biomarker profiling of heterogeneous circulating tumor cells using multifunctional nanospheres. *Anal. Chem.* **2018**, *90*, 10518−10526.

(20) Ding, C.; Zhang, C.; Yin, X.; Cao, X.; Cai, M.; Xian, Y. Near-infrared fluorescent Ag_2S nanodot-based signal amplification for efficient detection of circulating tumor cells. *Anal. Chem.* **2018**, *90*, 6702−6709.

(21) Osta, W. A.; Chen, Y.; Mikhitarian, K.; Mitas, M.; Salem, M.; Hannun, Y. A.; Cole, D. J.; Gillanders, W. E. EpCAM is overexpressed in breast cancer and is a potential target for breast cancer gene therapy. *Cancer Res.* **2004**, *64*, 5818−5824.

(22) Ignatiadis, M.; Kallergi, G.; Ntoulia, M.; Perraki, M.; Apostolaki, S.; Kafousi, M.; Chlouverakis, G.; Stathopoulos, E.; Lianidou, E.; Georgoulias, V.; Mavroudis, D. Prognostic value of the molecular detection of circulating tumor cells using a multimarker reverse transcription-PCR assay for cytokeratin 19, mammaglobin A, and HER2 in early breast cancer. *Clin. Cancer Res.* **2008**, *14*, 2593−2600.

(23) Maheswaran, S.; Sequist, L. V.; Nagrath, S.; Ulkus, L.; Brannigan, B.; Collura, C. V.; Inserra, E.; Diederichs, S.; Iafrate, A. J.; Bell, D. W.; Digumarthy, S.; Muzikansky, A.; Irimia, D.; Settleman, J.; Tompkins, R. G.; Lynch, T. J.; Toner, M.; Haber, D. A. Detection of mutations in EGFR in circulating lung-cancer cells. *N. Engl. J. Med.* **2008**, *359*, 366−377.

(24) Balasubramanian, S.; Kagan, D.; Hu, C. M. J.; Campuzano, S.; Lobo-Castanon, M. J.; Lim, N.; Kang, D. Y.; Zimmerman, M.; Zhang, L.; Wang, J. Micromachine-enabled capture and isolation of cancer cells in complex media. *Angew. Chem., Int. Ed.* **2011**, *50*, 4161−4164.

(25) Xie, M.; Lu, N.; Cheng, S.; Wang, X.; Wang, M.; Guo, S.; Wen, C.; Hu, J.; Pang, D.; Huang, W. Engineered decomposable multifunctional nanobioprobes for capture and release of rare cancer cells. *Anal. Chem.* **2014**, *86*, 4618−4626.

(26) Wen, C.-Y.; Wu, L.; Zhang, Z.; Liu, Y.; Wei, S.; Hu, J.; Tang, M.; Sun, E.; Gong, Y.; Yu, J.; Pang, D. Quick-response magnetic nanospheres for rapid, efficient capture and sensitive detection of circulating tumor cells. *ACS Nano* **2014**, *8*, 941−949.

(27) Cheng, S.-B.; Xie, M.; Chen, Y.; Xiong, J.; Liu, Y.; Chen, Z.; Guo, S.; Shu, Y.; Wang, M.; Yuan, B.; Dong, W.; Huang, W. Three-dimensional scaffold chip with thermosensitive coating for capture and reversible release of individual and cluster of circulating tumor cells. *Anal. Chem.* **2017**, *89*, 7924−7932.

(28) Labib, M.; Philpott, D. N.; Wang, Z.; Nemr, C.; Chen, J. B.; Sargent, E. H.; Kelley, S. O. Magnetic ranking cytometry: profiling rare cells at the single-cell level. *Acc. Chem. Res.* **2020**, *53*, 1445−1457.

(29) Jia, F.; Wang, Y.; Fang, Z.; Dong, J.; Shi, F.; Zhang, W.; Wang, Z.; Hu, Z. Novel peptide-based magnetic nanoparticle for mesenchymal circulating tumor cells detection. *Anal. Chem.* **2021**, *93*, 5670−5675.

(30) Zhou, X.; Zhang, Y.; Kang, K.; Mao, Y.; Yu, Y.; Yi, Q.; Wu, Y. Controllable environment protein corona-disguised immunomagnetic beads for high-performance circulating tumor cell enrichment. *Anal. Chem.* **2022**, *94*, 4650−4657.
(31) Allard, W. J.; Matera, J.; Miller, M. C.; Repollet, M.; Connelly, M. C.; Rao, C.; Tibbe, A. G. J.; Uhr, J. W.; Terstappen, L. W. M. M. Tumor cells circulate in the peripheral blood of all major carcinomas but not in healthy subjects or patients with nonmalignant diseases. *Clin. Cancer Res.* **2004**, *10*, 6897−6904.
(32) Sastre, J.; Maestro, M. L.; Puente, J.; Veganzones, S.; Alfonso, R.; Rafael, S.; Garci′a-Saenz, J. A.; Vidaurreta, M.; Marti′n, M.; Arroyo, M.; Sanz-Casla, M. T.; Di′az-Rubio, E. Circulating tumor cells in colorectal cancer: correlation with clinical and pathological variables. *Ann. Oncol.* **2008**, *19*, 935−938.
(33) Lai, C. H.; Lim, S. C.; Wu, L. C.; Wang, C. F.; Tsai, W. S.; Wu, H. C.; Chang, Y. C. Site-specific antibody modification and immobilization on a microfluidic chip to promote the capture of circulating tumor cells and microemboli. *Chem. Commun.* **2017**, *53*, 4152−4155.
(34) Lai, C. H.; Tsai, W. S.; Yang, M. H.; Chou, T. Y.; Chang, Y. C. A two-dimensional immunomagnetic nano-net for the efficient isolation of circulating tumor cells in whole blood. *Nanoscale* **2019**, *11*, 21119−21127.
(35) Thiery, J. P. Epithelial-mesenchymal transitions in tumour progression. *Nat. Rev. Cancer* **2002**, *2*, 442−454.
(36) Chaffer, C. L.; Weinberg, R. A. A perspective on cancer cell metastasis. *Science* **2011**, *331*, 1559−1564.
(37) Armstrong, A. J.; Marengo, M. S.; Oltean, S.; Kemeny, G.; Bitting, R. L.; Turnbull, J. D.; Herold, C. I.; Marcom, P. K.; George, D. J.; Garcia-Blanco, M. A. Circulating tumor cells from patients with advanced prostate and breast cancer display both epithelial and mesenchymal markers. *Mol. Cancer Res.* **2011**, *9*, 997−1007.
(38) Momburg, F.; Moldenhauer, G.; Hammerling, G. J.; Moller, P. Immunohistochemical study of the expression of a mr 34,000 human epithelium-specific surface glycoprotein in normal and malignant-tissues. *Cancer Res.* **1987**, *47*, 2883−2891.
(39) Li, Z.; Wang, G.; Shen, Y.; Guo, N.; Ma, N. DNA-templated magnetic nanoparticle-quantum dot polymers for ultrasensitive capture and detection of circulating tumor cells. *Adv. Funct. Mater.* **2018**, *28*, No. 1707152.
(40) Shen, Q.; Xu, L.; Zhao, L.; Wu, D.; Fan, Y.; Zhou, Y.; Ouyang, W. H.; Xu, X.; Zhang, Z.; Song, M.; Lee, T.; Garcia, M. A.; Xiong, B.; Hou, S.; Tseng, H. R.; Fang, X. Specific capture and release of circulating tumor cells using aptamer-modified nanosubstrates. *Adv. Mater.* **2013**, *25*, 2368−2373.
(41) Wang, X.; Qian, X.; Beitler, J. J.; Chen, Z. G.; Khuri, F. R.; Lewis, M. M.; Shin, H. J. C.; Nie, S.; Shin, D. M. Detection of circulating tumor cells in human peripheral blood using surface-enhanced Raman scattering nanoparticles. *Cancer Res.* **2011**, *71*, 1526−1532.
(42) Xie, H.-Y.; Xie, M.; Zhang, Z.; Long, Y.; Liu, X.; Tang, M.; Pang, D.; Tan, Z.; Dickinson, C.; Zhou, W. Wheat germ agglutinin-modified trifunctional nanospheres for cell recognition. *Bioconjugate Chem.* **2007**, *18*, 1749−1755.
(43) Tang, Y. H.; Lin, H. C.; Lai, C. L.; Chen, P. Y.; Lai, C. H. Mannosyl electrochemical impedance cytosensor for label-free MDA-MB-231 cancer cell detection. *Biosens. Bioelectron.* **2018**, *116*, 100−107.
(44) Ruiz-May, S. E.; Hucko, S.; Howe, K. J.; Zhang, S.; Sherwood, R. W.; Thannhauser, T. W.; Rose, J. K. C. A Comparative Study of Lectin Affinity Based Plant N-Glycoproteome Profiling Using Tomato Fruit as a Model. *Mol. Cell. Proteomics* **2014**, *13*, 566−579.
(45) Santos, A. F. S.; Silva, M. D. C.; da Napoleão, T. H.; Paiva, P. M. G.; Correia, M. T. S.; Coelho, L. C. B. B. Lectins: Function, structure, biological properties andpotential applications. *Curr. Top. Pept. Protein Res.* **2014**, *15*, 41−62.
(46) Tian, R.; Zhang, H.; Chen, H.; Liu, G.; Wang, Z. Uncovering the binding specificities of lectins with cells for precision colorectal cancer diagnosis based on multimodal imaging. *Adv. Sci.* **2018**, *5*, No. 1800214.
(47) Tian, R.; Zhao, S.; Liu, G.; Chen, H.; Ma, L.; You, H.; Liu, C.; Wang, Z. Construction of lanthanide-doped upconversion nanoparticle-Uelx Europaeus Agglutinin-I bioconjugates with brightness red emission for ultrasensitive in vivo imaging of colorectal tumor. *Biomaterials* **2019**, *212*, 64−72.
(48) Baldus, S. E.; Thiele, J.; Park, Y. O.; Hanisch, F. G.; Bara, J.; Fischer, R. Characterization of the binding specificity of Anguilla anguilla agglutinin (AAA) in comparison to Uelx europaeus agglutinin I (UEA-I). *Glycoconjugate J.* **1996**, *13*, 585−590.
(49) Chen, L.; Peng, M.; Li, N.; Song, Q.; Yao, Y.; Xu, B.; Liu, H.; Ruan, P. Combined use of EpCAM and FRa enables the high-efficiency capture of circulating tumor cells in non-small cell lung cancer. *Sci. Rep.* **2018**, *8*, No. 1188.
(50) Moriwaki, K.; Miyoshi, E. Fucosylation and gastrointestinal cancer. *World J. Hepatol.* **2010**, *2*, 151−161.

https://doi.org/10.1021/acsomega.2c03702
ACS Omega 2022, 7, 30405−30411